Bioorganic & Medicinal Chemistry xxx (2016) xxx–xxx

Contents lists available at ScienceDirect

Bioorganic & Medicinal Chemistry

journal homepage: www.elsevier.com/locate/bmc

Novel tricyclic pyrazolo[1,5-*d*][1,4]benzoxazepin-5(6*H*)-one: Design, synthesis, model and use as hMAO-B inhibitors

Rui Chen [a,†], Jie Xiao [c,†], Yong Ni [b], Han-Fei Xu [b], Min Zheng [b], Xu Tong [a], Tong-Tian Zhang [a], Chenzhong Liao [b,*], Wen-Jian Tang [a,*]

[a] School of Pharmacy, Anhui Medical University, Hefei 230032, PR China
[b] School of Medical Engineering, Hefei University of Technology, Hefei 230009, PR China
[c] School of Pharmacy, Anhui University of Chinese Medicine, Hefei 230012, PR China

ARTICLE INFO

Article history:
Received 18 January 2016
Revised 26 February 2016
Accepted 29 February 2016
Available online xxxx

Keywords:
hMAO
Isoform selectivity
Benzoxazepinone
Selective hMAO-B inhibitor
Anti-Parkinson

ABSTRACT

Based on our recently reported selective hMAO-A inhibitors, on which, the intramolecular cyclization led to a very interesting change of isoform selectivity. A series of selective hMAO-B inhibitors (**3a**–**3u**) with novel scaffold of tricyclic pyrazolo[1,5-*d*][1,4]benzoxazepin-5(6*H*)-one were designed and synthesized. Compound **3u** (IC_{50} = 221 nM) exhibited the best inhibitory activity and isoform selectivity against hMAO-B, superior to selegiline (IC_{50} = 321 nM), which is a commercial selective hMAO-B inhibitor used to Parkinson's disease. Modeling study indicated that the selectivity of our compounds to hMAO-B is determined by at least two residues, i.e., Ile 199 and Cys 172 (or corresponded Phe 208 and Asn 181 of hMAO-A). These data support further studies to assess rational design of more efficiently selective hMAO-B inhibitors.

1. Introduction

Monoamine oxidases (MAO, EC 1.4.3.4) are flavin-containing amine oxidoreductases bound to the mitochondrial outer membrane, which play essential roles in the catabolism of amine neurotransmitters in the peripheral and central nervous systems.[1,2] The human monoamine oxidases mainly have two isoforms, namely hMAO-A and hMAO-B, with different three-dimensional structures, substrate specificity and inhibitor selectivity. hMAO-A has more specific for serotonin and noradrenaline, while hMAO-B preferentially deaminates phenylethylamine and benzylamine. Tyramine, tryptamine and dopamine are common substrates for both isoforms.[3,4] Although both isoforms exhibit high sequence homology, they differ in shapes and volumes of the catalytic sites allowed to discovery selective inhibitors.

MAO inhibitors have been showed to have potential uses in the treatment of psychiatric and neurological diseases. The first generation MAO inhibitors were introduced into clinical use as antidepressants, however, many nonselective and irreversible MAO inhibitors were withdrawn from the clinic due to serious side effects such as liver toxicity and hypertensive crisis.[5]

The reversible and selective hMAO inhibitors resulted in improved safety profile and in renewed interests for the development of novel selective MAO inhibitors. Actually, hMAO-A inhibitors mainly act as antidepressant and anti-anxiety agents, whereas hMAO-B inhibitors are used alone or in combination to treat Alzheimer's (AD) and Parkinson's (PD) diseases.[6–8] hMAO-B elevation in PD patients may lead to an increased production of hydrogen peroxide and other reactive oxygen species (ROS), responsible for neuron degeneration. MAO-B-mediated ROS contributes to neuropathology and antioxidant treatment can arrest further progression of dopaminergic cell death.[9,10] Thus, neurological degeneration in the central nervous system could be associated to the oxidative stress, and with an increased MAO-B activity. Therefore, hMAO-B represents an attractive target for the treatment of the neurodegenerative diseases, including PD.[11] Two selective hMAO-B inhibitors, selegiline and rasagiline are marketed drugs for the treatment of PD. But both are irreversible hMAO inhibitors, which utilize the propargyl group to covalently bind to the flavin ring of the cofactor, flavin adenine dinucleotide (FAD). In this way, the bound enzymes could not work and thus enzyme activity was blocked until the cell makes new enzymes.

Both of AD and PD are related with elevated levels of hMAO-B in the brain, therefore, novel, potent, selective and reversible hMAO-B

* Corresponding authors. Tel./fax: +86 551 62901285 (C.L.), +86 551 65161115 (W.-J.T.).
E-mail addresses: czliao@hfut.edu.cn (C. Liao), ahmupharm@126.com (W.-J. Tang).
† These authors contributed equally to this work.

http://dx.doi.org/10.1016/j.bmc.2016.02.045
0968-0896/

inhibitors have gained considerable attentions in the treatment of these two diseases and other disorders.[11] The development of synthetic heterocyclic compounds as MAOIs progressed considerably during the past decade. Different families of heterocycles containing nitrogen atoms have been used as scaffolds for the discovery of selective and reversible hMAO inhibitors.[12–19]

Recently, we identified 3,5-diaryl-2-pyrazoline-1-ethanone derivatives as potent and selective hMAO-A inhibitors.[20] In this work, we reported selective hMAO-B inhibitors (**3a**–**3u**) with a novel scaffold of tricyclic pyrazolo[1,5-*d*][1,4]benzoxazepin-5(6*H*)-one, which was derived from the selective hMAO-A inhibitors mentioned above[20] by the intramolecular cyclization of 1-ethanone bromide with hydroxyl group. This cyclization led to a very interesting change of isoform selectivity from hMAO-A to hMAO-B. Amongst them, compound **3u** (IC_{50} = 221 nM) exhibited the best inhibitory activity and isoform selectivity against hMAO-B, superior to selegiline (IC_{50} = 321 nM), a selective hMAO-B inhibitor currently in the market for the treatment of Parkinson's disease. Further molecular modeling demonstrates that the selectivity of our compounds to hMAO-B is determined by at least two residues, i.e., Ile 199 and Cys 172 of hMAO-B (or corresponded Phe 208 and Asn 181 of hMAO-A).

2. Results and discussion

2.1. Inhibitor design

Based on our recently reported 3,5-diaryl-2-pyrazoline-1-ethanone derivatives as selective hMAO-A inhibitors,[20] on which, the intramolecular cyclization of ethanone bromide with hydroxyl group produced a novel scaffold of tricyclic pyrazolo[1,5-*d*][1,4] benzoxazepin-5(6*H*)-one derivatives (Fig. 1). The novel scaffold could be nicely docked into the active site of hMAO-B, indicating they have the potential to be developed as hMAO-B inhibitors. Therefore, we synthesized a series of compounds (**3a**–**3u**) containing this scaffold. Interestingly, this intramolecular cyclization did result in the change of isoform selectivity from hMAO-A to hMAO-B, most of them showed reversible and selective hMAO activity, for example, compound **3u** did not show any activity against hMAO-A, but had an IC_{50} value of 221 nM against hMAO-B, superior to selegiline (IC_{50} = 321 nM).

2.2. Chemistry

Pyrazolo[1,5-*d*][1,4]benzoxazepin-5(6*H*)-one derivatives (**3a**–**3u**, as shown in Table 1) were synthesized according to the protocol outlined in Scheme 1. After styrene ketones were prepared through Claisen–Schmidt condensation of substituted salicylaldehyde with acetophenone, the key intermediate 2-pyrazoline derivatives (**1**) were synthesized by the cyclization reaction of excess hydrazine hydrate with the styrene ketones. The 2-pyrazoline-1-ethanone derivatives (**2**) were obtained through the acylation of compound **1** with α-bromoacyl chloride. The title compounds **3a**–**3u** were obtained from the cyclization reaction of compound **2** in the present of $NaHCO_3$ catalysis in ethanol.[20,21]

2.3. Crystal structure analysis

The structures of compounds **3e**, **3m** and **3t** were determined by X-ray crystallography. Crystal data of compound **3e**: Colorless plate crystals, yield, 87%; mp 168–169 °C; $C_{17}H_{13}ClN_2O_2$, *Mr* = 312.74, Monoclinic, space group $P_{121/c1}$; *a* = 13.3672(9), *b* = 14.2568(10), *c* = 7.7793(6) (Å); α = 90, β = 97.002(7), γ = 90, *V* = 1471.49(19) Å^3, *T* = 293(2) K, *Z* = 4, *Dx* = 1.412 g/cm^3, *F*(000) = 648.0, Reflections collected/independent reflections = 2891/1988, Data/restraints/parameters = 2891/0/199, Goodness of fit on F^2 = 1.053, Fine, R_1 = 0.0506, $wR(F^2)$ = 0.1242. Compound **3m**: Colorless block crystals, yield, 47%; mp 224–225 °C; $C_{17}H_{12}ClFN_2O_2$, *M* = 348.75, Monoclinic, space group $I_{12/a1}$; *a* = 12.7349(3), *b* = 17.3453(4), *c* = 14.6200(3) (Å); α = 90, β = 103.788(2), γ = 90, *V* = 3136.37(12) Å^3, *T* = 291(10) K, *Z* = 8, D_{calcd} = 1.477 g/cm^3, *F*(000) = 1440, Reflections collected/independent reflections = 2903/2565, Data/restraints/parameters = 2903/0/221, Goodness of fit on F^2 = 1.036, Fine, R_1 = 0.0981, $wR(F^2)$ = 0.1018. Compound **3t**: Colorless plate crystals, yield, 50%; mp 173–175 °C; $C_{18}H_{15}ClN_2O_2$, *M* = 326.77, Triclinic, space group P_{-1}; *a* = 5.1296(2), *b* = 9.5222(5), *c* = 16.1436(8) (Å); α = 79.376(4), β = 87.744(4), γ = 88.468(4), *V* = 774.27(7) Å^3, *T* = 292(2) K, *Z* = 2, D_{calcd} = 1.402 g/cm^3, *F*(000) = 340.0, Reflections collected/independent reflections = 2773/2582, Data/restraints/parameters = 2773/0/209, Goodness of fit on F^2 = 1.063, Fine, R_1 = 0.0346, $wR(F^2)$ = 0.0985.

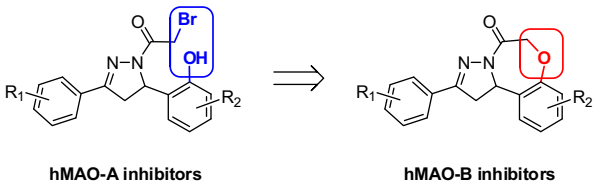

Figure 1. The general inhibitor design strategy in this study.

The molecular structures of compounds **3e**, **3m** and **3t** are shown in Figure 2. Crystallographic data (excluding structure factors) for the structures have been deposited in the Cambridge Crystallographic Data Center as supplementary publication Nos. CCDC 1428287, 1040100 and 1040101.

2.4. Inhibition against hMAO-A and hMAO-B

The potential inhibitory activities of the synthesized compounds **3a**–**3u** against hMAO-A and hMAO-B were investigated by measuring their effects on the production of hydrogen peroxide (H_2O_2) from *p*-tyramine, using the Amplex Red MAO assay kit (Molecular Probes, Inc., Eugene, Oregon, USA) and MAO isoforms in microsomes prepared from insect cells infected with Recombinant baculovirus containing cDNA inserts for hMAO-A or hMAO-B. The inhibition of hMAO activity was evaluated using the general method described by Santana et al.[22] The test compounds did not show any interference with the reagents used for a biochemical assay. The results of hMAO-A and hMAO-B inhibition studies with title compounds are showed in Table 1 together with the hMAO-B selectivity index ([IC_{50}(hMAO-A)]/[IC_{50}(hMAO-B)]). An irreversible and selective hMAO-A inhibitor, clorgyline and an irreversible and selective hMAO-B inhibitor, selegiline were employed as the positive control compounds in this test.

Enzymatic assays revealed that most of tested compounds exhibited inhibitory activities against hMAO, and showing selectivity toward hMAO-B. It is obvious from the data that compounds **3m** and **3u** exhibited the best activities against hMAO-B with IC_{50} values of 242 and 221 nM, respectively, surpassing that of the positive control selegiline (IC_{50} = 321 nM).[23] Besides the most potent inhibitory activity, compound **3u** (IC_{50} = 221 nM) also showed the highest selectivity (271.1-fold) with respect to the hMAO-B isoform. Inspection of the chemical structures, it can be concluded that among the synthesized compounds, the hMAO-B inhibitory activity was affected by the substituent groups at C2, C6 positions and the benzene ring of benzoxazepinone moiety (Table 1). Further, the substituent on the benzene ring connected to the pyrazole ring had impact on both of hMAO-A and hMAO-B inhibition.

Table 1
The chemical structures of compounds **3a**–**3u** and their inhibitory activities and selectivities against hMAO-A and hMAO-B[a]

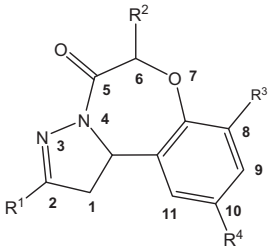

Compd	R_1	R_2	R_3	R_4	MAO-A (nM)	MAO-B (nM)	SI MAO-B[c]
3a	4-CH_3O-Ph	H	H	H	[b]	[b]	–
3b	Ph	H	H	H	2195 ± 175	2878 ± 213	0.8
3c	4-*i*-Pr-Ph	H	H	H	[b]	3522 ± 184	17.0
3d	4-CH_3-Ph	H	H	H	[b]	[b]	–
3e	4-Cl-Ph	H	H	H	53260 ± 2230	[b]	0.9
3f	4-F-Ph	H	H	H	[b]	1782 ± 126	33.7
3g	2-Cl-Ph	H	H	H	55680 ± 2540	1321 ± 120	42.1
3h	2-CH_3-Ph	H	H	H	[b]	[b]	–
3i	4-CH_3O-Ph	H	H	Cl	[b]	2722 ± 189	22.0
3j	4-CH_3-Ph	H	H	Cl	3904 ± 154	1634 ± 86	2.4
3k	Ph	H	H	Cl	[b]	2568 ± 98	23.4
3l	4-Cl-Ph	H	H	Cl	4712 ± 172	504 ± 56	9.3
3m	4-F-Ph	H	H	Cl	4654 ± 89	242 ± 27	19.2
3n	2-F-Ph	H	H	Cl	[b]	584 ± 95	102.7
3o	4-CH_3O-Ph	H	Br	Br	4756 ± 215	467 ± 22	10.2
3p	4-CH_3O-Ph	CH_3	H	H	[b]	[b]	–
3q	4-CH_3-Ph	CH_3	H	H	[b]	45240 ± 2680	1.3
3r	Ph	CH_3	H	H	[b]	34670 ± 2030	1.7
3s	4-Cl-Ph	CH_3	H	H	[b]	452 ± 26	132.7
3t	2-Cl-Ph	CH_3	H	H	4055 ± 122	348 ± 104	11.7
3u	4-F-Ph	CH_3	H	H	[b]	221 ± 28	271.1
Clorgyline					189 ± 7	[b]	0.0031
Selegiline					[b]	321 ± 11	187.0

[a] Each IC_{50} value is the mean ± SEM from three experiments ($n = 3$).
[b] Inactive at 60 μM, IC_{50} values obtained under the assumption that the corresponding IC_{50} against either hMAO-A or hMAO-B is the highest concentration tested.
[c] SI MAO-B = [IC_{50}(MAO-A)]/[IC_{50}(MAO-B)].

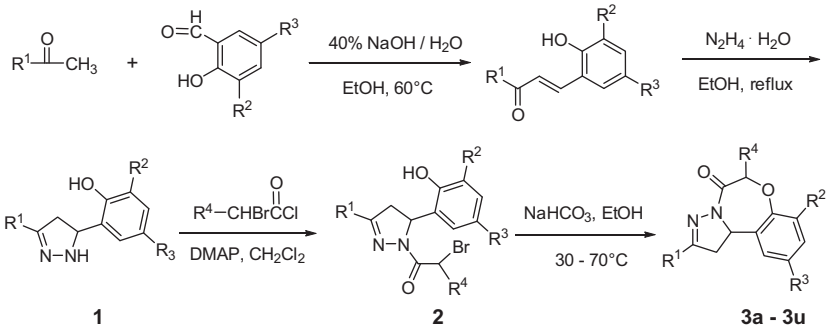

Scheme 1. Synthesis of pyrazolo[1,5-*d*][1,4]benzoxazepin-5(6*H*)-one derivatives **3a**–**3u**.

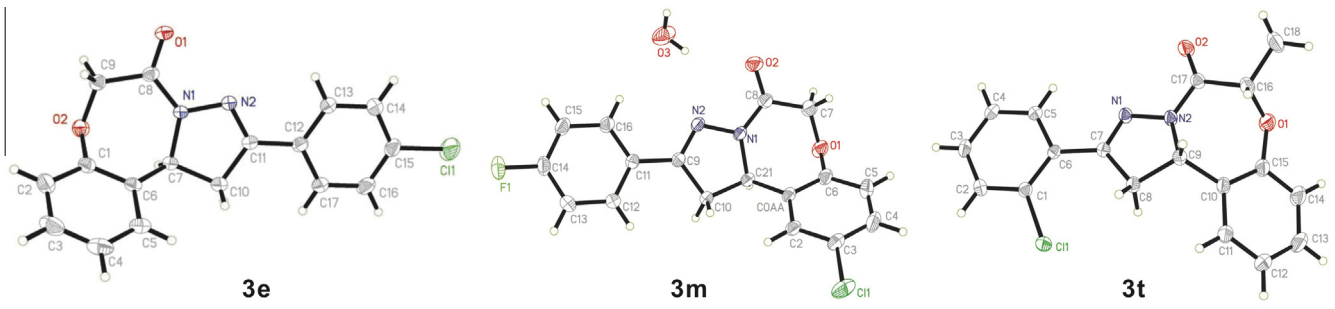

Figure 2. An ORTEP view of the molecular structures of compounds **3e**, **3m** and **3t**.

Compounds with halogen substituents at the benzene ring in the benzoxazepinone moiety have great influence on the hMAO-B inhibition, for example, compounds **3i**–**3n** with 10-chloro substitution at the benzene ring were found better in terms of potency than the corresponding compounds **3a**–**3h** without the substituents. Compound **3o** with 8,10-dibromo substituents showed more potent hMAO-B inhibitory activity (IC_{50} = 467 nM) than the monochloro substituted compound **3i** (IC_{50} = 2722 nM) and the compound without substitution **3a** (IC_{50} > 60 μM). This trend can also be observed among compounds **3b**, **3k**, compounds **3d**, **3j**, compounds **3f**, **3m**, and compounds **3e**, **3l**, etc.

From Table 1, it is intuitive that the volumes of the *para*-substituted groups at the benzene ring in the C2 position have influences on the activity. For hMAO-B, the smaller of this substituent, the better of the inhibitory activity. The methyl group at the R2 position also has great impact on the inhibitory activity against hMAO: it can increase the potency against B-isoform but retard the potency against A-isoform. For example, compound **3f** has an IC_{50} value of 1782 nM against hMAO-B; when the R2 position is methyl (compound **3u**), the IC_{50} value was changed to 221 nM, having an 8-fold increment.

2.5. Molecular docking study

Structure-based docking methods have been successfully employed to detect the binding poses and energies of small ligands to their receptors.[24] To explore the binding models of the compounds discussed herein to hMAO-B, explain the SAR and isoform selectivity between hMAO-A and hMAO-B and further guide the design of more potent and specific hMAO-B inhibitors, these compounds were docked into the active site of hMAO-B using Glide 5.9 of the Schrödinger suite. The standard precision (SP) of Glide[25] was employed. The PDB code used of the hMAO-B complex was 2V5Z which has an X-ray resolution of 1.6 Å and a *R*-factor of 0.227.[13] In this complex, a selective non-covalent inhibitor resides in the binding pocket. During the docking process, the thiol group of Cys 172 was allowed to adopt different orientations since in the crystal structure of 2V5Z, an intramolecular hydrogen bond between this thiol group and the protein can be observed, however, in the crystal structure of 2XFQ,[26] this hydrogen bond does not exist.

Among the many docking poses produced by Glide SP, a pose having a score of −9.896 kJ/mol of compound **3u** can explain the SAR and selectivity of our compounds to both hMAO-A and hMAO-B very well. From the docking pose of compound **3u** to hMAO-B, it can be seen that this compound fills the binding pocket of hMAO-B very well, mainly forming hydrophobic interactions with surrounding hydrophobic residues (Fig. 3A and B). Furthermore, a hydrogen bond can be observed in the docking complex of compound **3u** to hMAO-B.

The benzene ring in the benzoxazepinone moiety is in the hydrophobic sub-pocket composed of Leu 171, Tyr 326, Leu 328, Tyr 398 and Phe 343, so increasing both of the hydrophobicity and volume may enhance the inhibition against hMAO-B. It is well known that halogen atoms can increase the hydrophobicity and volume and therefore they have wide applications in medicinal chemistry.[27] Indeed, when one or two hydrogen atoms in this benzene ring were substituted by halogens, such as chlorine or bromine, the binding affinities were enhanced a lot. For hMAO-B, compound **3a** had no inhibition against hMAO-B even at 60 μM, however, when R4 was chlorine (compound **3i**, see Table 1), the IC_{50} was 2722 nM; when both R3 and R4 were bromine (compound **3o**), the IC_{50} was dramatically changed to 467 nM. This trend also can be observed among compounds **3b**, **3k**, compounds **3d**, **3j**, compounds **3f**, **3m**, and compounds **3e**, **3l**, etc. For the corresponding sub-pocket in hMAO-A, because the residues are same as the ones in hMAO-B, this trend also can be perceived, although the inhibitions against hMAO-A were much lower or even lost. In the docking pose of compound **3u** to hMAO-B, another benzene ring connected to the pyrazole moiety inserts into a hydrophobic sub-pocket and has hydrophobic interactions with the surrounding residues such as Phe 168, Leu 171, Ile 199, Ile 316 and Tyr 326. Increasing the volume of this benzene ring may attenuate the inhibition against hMAO-B, for example, the IC_{50} of compound **3b** was 2878 nM, however, when the hydrogen atom at the para-position was replaced by bulky groups (see compounds **3a**, **3d**, **3e**), the binding affinities dropped. Since fluorine atom has a similar VDW radius as hydrogen atom and it can increase the hydrophobicity of benzene, it is not surprised to see that compound **3f** had better IC_{50} against hMAO-B than compound **3b**.

Almost of all compounds discussed herein showed no activity against hMAO-A, which is also explainable from the docking pose of compound **3u**: when superimposing the crystal structure of

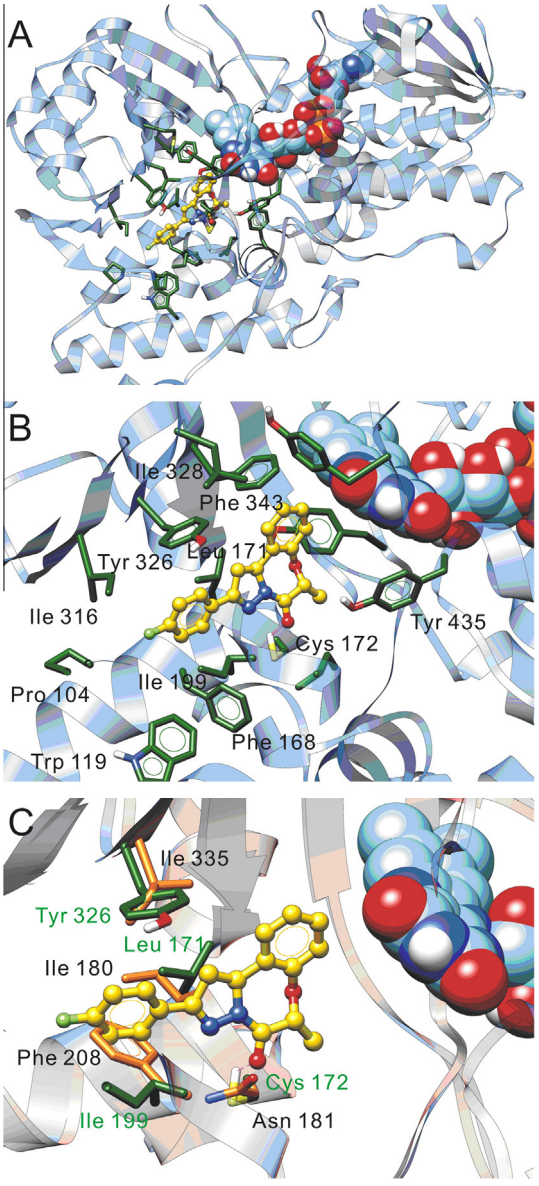

Figure 3. Putative binding pose of compound **3u** to hMAO-B. (A) Ribbon diagram of the docked complex of **3u** (yellow) to hMAO-B. The FAD is represented as a sphere model. (B) The residues of hMAO-B around the docked compound **3u**. A hydrogen bond between **3u** and Cys 172 is indicated by a magenta dashed line. (C) The different residues between hMAO-A (orange) and hMAO-B (green) around the docking pose of compound **3u**.

hMAO-A (PDB code: 2Z5X[28]) with our docking complex of hMAO-B, it can be seen that in hMAO-A, the corresponding residue of Ile 199 of hMAO-B is Phe 208, which would have conflicts with our compounds (see Fig. 3C) and therefore dramatically reduce the inhibition against hMAO-A or do not inhibit hMAO-A at all. It is interesting to notice that the carbonyl group of compound **3u** can form a hydrogen bond with the residue of Cys 172 of hMAO-B. Nevertheless, in this corresponding position in hMAO-A, the residue is Asn 181, which could not form a hydrogen bond with the carbonyl group. We can see that in compounds **3p**–**3u**, there is an extra methyl group in the R2 position, which is close to the carbonyl group. This methyl group may have extra hydrophobic interactions with the residue of Tyr 398 and Cys 172 in hMAO-B, as indicated by the docking study, which can explain why compounds **3p**–**3u** had better inhibitions than the corresponding compounds without the methyl group. However, in hMAO-A, the corresponding residue of Cys 172 of hMAO-B is Asn 181, which would have conflict with the methyl group and cause worse inhibition. Residue of Tyr 326 of hMAO-B is close to the docked pose of compound **3u**, and has hydrophobic interaction with it. In hMAO-A, the equivalent residue is Ile 335, which is smaller than Tyr. Another different residue around the docked compound is Leu 171 of hMAO-B and corresponding Ile 180 of hMAO-A. Both of these two residues may also have impacts on the isoform selectivity.

Since all compounds discussed herein did not show inhibitions or showed very weak activities against hMAO-A, it is not meaningful to try to identify the docking pose of these weak inhibitors to hMAO-A using docking methods.

All in all, we can see that the selectivity of our compounds to hMAO-B is determined by at least two residues, i.e., Ile 199 and Cys 172 of hMAO-B (or corresponded Phe 208 and Asn 181 of hMAO-A). A- and B-isoforms of h-MAO share about 70% sequence identities; in the binding pockets, only few residues between them are different. Employing the difference of the residues in the binding pockets of hMAO-A and hMAO-B, it is feasible to design and identify isoform selective hMAO inhibitors.

3. Conclusion

In this work, based on our recently reported selective hMAO-A inhibitors,[19] a series of selective hMAO-B inhibitors (**3a**–**3u**) with a novel scaffold of tricyclic pyrazolo[1,5-*d*][1,4]benzoxazepin-5(6*H*)-one were designed and synthesized. Compared with our early reported of selective hMAO-A inhibitors, the intramolecular cyclization led to this interesting change of isoform selectivity. Compound **3u** (IC_{50} = 221 nM) exhibited best inhibitory activity and isoform selectivity against hMAO-B, better than selegiline (IC_{50} = 321 nM). Further docking study shows that the selectivity of our compounds to hMAO-B is determined by at least two residues, i.e., Ile 199 and Cys 172 (or corresponded Phe 208 and Asn 181 of hMAO-A). Two other residues, i.e., Tyr 326 and Leu 171 of hMAO-B, may also have impacts on the selectivity. This striking selectivity profile of compounds reported herein imply that we can further develop selective hMAO-B and/or hMAO-A inhibitors based on this novel scaffold using a diversity evolution strategy.[29]

4. Experimental section

4.1. Chemicals and instrumentation

All starting materials, unless noted elsewhere, were obtained from commercial companies and were used without purification. The reactions were monitored by thin layer chromatography (TLC) on pre-coated silica GF_{254} plates. Melting points (mp) were determined on a XT4MP apparatus (Taike Corp., Beijing, China) and are uncorrected. Proton (^{1}H) and carbon (^{13}C) NMR spectra were recorded in $CDCl_3$ or DMSO-d_6 on a Bruker AV300 spectrometer at frequencies of 300 MHz and 75 MHz, respectively. Chemical shifts are reported in parts per million (δ) downfield from the signal of TMS as internal standards. Spin multiplicities are given as s (singlet), d (doublet), t (triplet), q (quartet) or m (multiplet). High resolution mass spectra (HRMS) were obtained on an Agilent 1260-6221 TOF mass spectrometry.

4.2. Procedures for the synthesis of title compounds 3a–3u

To a solution of aromatic methyl ketones (10 mmol) and salicylaldehyde (11 mmol) in ethanol (10 mL) was added 40% NaOH aqueous solution (2 mL) dropwise and the reaction was carried out at 60 °C for 4–10 h until the disappearance of starting material (monitored by TLC). The mixture was poured into cold water and neutralized with 2 M HCl to a pH in the range of 2–3. The resulting precipitate was collected, washed with water and dried to give chalcones. The chalcone was treated with 5 times excess of hydrazine hydrate in dry ethanol and refluxed for 3–6 h. The reaction mixture was then poured into ice-cold water. The solid was filtered, washed and recrystallized from ethanol to afford respective pyrazoline (**1**). A mixture of compound **1** and α-bromoacyl chloride in CH_2Cl_2 was added 4-dimethylaminopyridine (DMAP) and the reaction was stirred overnight. The reaction mixture was washed with water and brine, dried with anhydrous Na_2SO_4, filtrated and concentrated in vacuo. The resulting residue was then purified by column chromatography to give the *N*-acylated product **2**. $NaHCO_3$ (3.0 mmol) was added to an ethanol (20 mL) solution of compound **2** (2.0 mmol), then the reaction mixture was stirred at 30 °C until the disappearance of starting material (monitored by TLC). EtOAc (100 mL) was added to the reaction mixture, then washed with water and brine, dried with anhydrous Na_2SO_4, filtrated and concentrated in vacuo. The residue was purified by chromatography on a silica gel column (petroleum/EtOAc, 1:1 → 1:2) to give title compounds **3a**–**3u**.

4.2.1. 2-(4-Methoxy-phenyl)-1,11b-dihydro-pyrazolo[1,5-*d*][1,4]benzoxazepin-5(6*H*)-one (3a)

The title compound was prepared from 4-methoxy-phenyl methyl ketone and salicylaldehyde in a yield of 19%: white powder; mp 231–233 °C; ^{1}H NMR (300 MHz, DMSO-d_6) δ (ppm): 3.73–3.88 (m, 4H, CH_3O, 1-Ha), 3.97 (dd, 1H, J_1 = 9.1 Hz, J_2 = 17.9 Hz, pyrazole 1-Hb), 4.36 (d, 1H, J = 16.0 Hz, 6-Ha), 5.01 (d, 1H, J = 16.0 Hz, 6-Hb), 6.02 (dd, 1H, J_1 = 8.8 Hz, J_2 = 11.3 Hz, 11b-H), 7.03–7.85 (8H, Ar-H). TOF-HRMS: m/z $[M+H]^+$ calcd for $C_{18}H_{17}N_2O_3$: 309.1234; found: 309.1233.

4.2.2. 2-Phenyl-1,11b-dihydro-pyrazolo[1,5-*d*][1,4]benzoxazepin-5(6*H*)-one (3b)

The title compound was prepared from phenyl methyl ketone and salicylaldehyde in a yield of 22%: white powder; mp 191–193 °C; ^{1}H NMR (300 MHz, $CDCl_3$) δ (ppm): 3.69 (dd, 1H, J_1 = 11.5 Hz, J_2 = 17.4 Hz, 1-Ha), 3.92 (dd, 1H, J_1 = 9.3 Hz, J_2 = 17.4 Hz, 1-Hb), 4.48 (d, 1H, J = 16.7 Hz, 6-Ha), 5.05 (d, 1H, J = 16.7 Hz, 6-Hb), 6.01 (dd, 1H, J_1 = 8.8 Hz, J_2 = 11.3 Hz, 11b-H), 7.17–8.03 (9H, Ar-H); ^{13}C NMR (75 MHz, $CDCl_3$) δ (ppm): 35.4 (1-C), 56.3 (11b-C), 72.9 (6-C), 121.4, 124.6, 125.2, 127.3 (2C), 128.7 (2C), 130.6, 130.7, 130.8, 131.0, 156.1 (2-C), 158.0, 164.7. TOF-HRMS: m/z $[M+H]^+$ calcd for $C_{17}H_{15}N_2O_2$: 279.1128; found: 279.1127.

4.2.3. 2-(4-Isopropyl-phenyl)-1,11b-dihydro-pyrazolo[1,5-*d*][1,4]benzoxazepin-5(6*H*)-one (3c)

The title compound was prepared from 4-isopropyl-phenyl methyl ketone and salicylaldehyde in a yield of 18%: white powder; mp 180–181 °C; ^{1}H NMR (300 MHz, $CDCl_3$) δ (ppm): 1.28 (d,

6H, J = 6.9 Hz), 2.97 (dt, 1H, J_1 = 6.9 Hz, J_2 = 13.8 Hz, CH), 3.67 (dd, 1H, J_1 = 11.5 Hz, J_2 = 17.3 Hz, 1-Ha), 3.90 (dd, 1H, J_1 = 9.2 Hz, J_2 = 17.3 Hz, 1-Hb), 4.47 (d, 1H, J = 16.7 Hz, 6-Ha), 5.04 (d, 1H, J = 16.7 Hz, 6-Hb), 6.00 (dd, 1H, J_1 = 9.5 Hz, J_2 = 11.1 Hz, 11b-H), 7.18–7.93 (8H, Ar-H); ^{13}C NMR (75 MHz, $CDCl_3$) δ (ppm): 23.8 (2C), 34.2 (CH), 35.4 (1-C), 56.1 (11b-C), 72.9 (6-C), 121.4, 124.6, 125.2, 126.8 (2C), 127.5 (2C), 128.1, 130.6, 130.9, 152.3, 156.1 (2-C), 158.0, 164.5. TOF-HRMS: m/z $[M+H]^+$ calcd for $C_{20}H_{21}N_2O_2$: 321.1598; found: 321.1598.

4.2.4. 2-*p*-Tolyl-1,11b-dihydro-pyrazolo[1,5-*d*][1,4]benzoxazepin-5(6*H*)-one (3d)

The title compound was prepared from *p*-methyl-phenyl methyl ketone and salicylaldehyde in a yield of 23%: white powder; mp 252–253 °C; ^{1}H NMR (300 MHz, $CDCl_3$) δ (ppm): 2.41 (s, 3H, CH_3), 3.66 (dd, 1H, J_1 = 11.4 Hz, J_2 = 17.3 Hz, 1-Ha), 3.90 (dd, 1H, J_1 = 9.3 Hz, J_2 = 17.3 Hz, 1-Hb), 4.47 (d, 1H, J = 16.7 Hz, 6-Ha), 5.04 (d, 1H, J = 16.7 Hz, 6-Hb), 5.99 (dd, 1H, J_1 = 9.6 Hz, J_2 = 11.1 Hz, 11b-H), 7.19–7.90 (8H, Ar-H). TOF-HRMS: m/z $[M+H]^+$ calcd for $C_{18}H_{17}N_2O_2$: 293.1285; found: 293.1294.

4.2.5. 2-(4-Chloro-phenyl)-1,11b-dihydro-pyrazolo[1,5-*d*][1,4]benzoxazepin-5(6*H*)-one (3e)

The title compound was prepared from 4-chloro-phenyl methyl ketone and salicylaldehyde in a yield of 18%: white powder; mp 250–251 °C; ^{1}H NMR (300 MHz, $CDCl_3$) δ (ppm): 3.65 (dd, 1H, J_1 = 11.5 Hz, J_2 = 17.4 Hz, 1-Ha), 3.90 (dd, 1H, J_1 = 9.4 Hz, J_2 = 17.4 Hz, 1-Hb), 4.47 (d, 1H, J = 16.7 Hz, 6-Ha), 5.04 (d, 1H, J = 16.7 Hz, 6-Hb), 6.02 (dd, 1H, J_1 = 9.6 Hz, J_2 = 11.1 Hz, 11b-H), 7.19–7.94 (8H, Ar-H). TOF-HRMS: m/z $[M+H]^+$ calcd for $C_{17}H_{14}ClN_2O_2$: 313.0738; found: 313.0735.

4.2.6. 2-(4-Fluoro-phenyl)-1,11b-dihydro-pyrazolo[1,5-*d*][1,4]benzoxazepin-5(6*H*)-one (3f)

The title compound was prepared from 4-fluoro-phenyl methyl ketone and salicylaldehyde in a yield of 20%:, white powder; mp 229–230 °C; ^{1}H NMR (300 MHz, $CDCl_3$) δ (ppm): 3.66 (dd, 1H, J_1 = 11.5 Hz, J_2 = 17.3 Hz, 1-Ha), 3.90 (dd, 1H, J_1 = 9.4 Hz, J_2 = 17.3 Hz, 1-Hb), 4.48 (d, 1H, J = 16.7 Hz, 6-Ha), 5.05 (d, 1H, J = 16.7 Hz, 6-Hb), 6.00 (dd, 1H, J_1 = 9.6 Hz, J_2 = 11.1 Hz, 11b-H), 7.19–7.99 (8H, Ar-H). TOF-HRMS: m/z $[M+H]^+$ calcd for $C_{17}H_{14}FN_2O_2$: 297.1034; found: 297.1033.

4.2.7. 2-(2-Chloro-phenyl)-1,11b-dihydro-pyrazolo[1,5-*d*][1,4]benzoxazepin-5(6*H*)-one (3g)

The title compound was prepared from 2-chloro-phenyl methyl ketone and salicylaldehyde in a yield of 26%: white powder; mp 160–162 °C; ^{1}H NMR (300 MHz, $CDCl_3$) δ (ppm): 3.86 (dd, 1H, J_1 = 11.3 Hz, J_2 = 17.9 Hz, 1-Ha), 4.15 (dd, 1H, J_1 = 9.5 Hz, J_2 = 17.9 Hz, 1-Hb), 4.49 (d, 1H, J = 16.7 Hz, 6-Ha), 5.06 (d, 1H, J = 16.7 Hz, 6-Hb), 6.03 (dd, 1H, J_1 = 9.5 Hz, J_2 = 11.4 Hz, 11b-H), 7.20–7.97 (8H, Ar-H). TOF-HRMS: m/z $[M+H]^+$ calcd for $C_{17}H_{14}ClN_2O_2$: 313.0738; found: 313.0738.

4.2.8. 2-*o*-Tolyl-1,11b-dihydro-pyrazolo[1,5-*d*][1,4]benzoxazepin-5(6*H*)-one (3h)

The title compound was prepared from *o*-methyl-phenyl methyl ketone and salicylaldehyde in a yield of 22%: yellow powder; mp 180–182 °C; ^{1}H NMR (300 MHz, $CDCl_3$) δ (ppm): 2.67 (s, 3H, CH_3), 3.71 (dd, 1H, J_1 = 11.4 Hz, J_2 = 17.3 Hz, 1-Ha), 3.95 (dd, 1H, J_1 = 9.3 Hz, J_2 = 17.3 Hz, 1-Hb), 4.48 (d, 1H, J = 16.7 Hz, 6-Ha), 5.05 (d, 1H, J = 16.7 Hz, 6-Hb), 5.96 (dd, 1H, J_1 = 9.5 Hz, J_2 = 11.1 Hz, 11b-H), 7.18–7.58 (8H, Ar-H). TOF-HRMS: m/z $[M+H]^+$ calcd for $C_{18}H_{17}N_2O_2$: 293.1285; found: 293.1291.

4.2.9. 10-Chloro-2-(4-methoxy-phenyl)-1,11b-dihydro-pyrazolo[1,5-*d*][1,4]benzoxazepin-5(6*H*)-one (3i)

The title compound was prepared from 4-methoxy-phenyl methyl ketone and 5-chloro-salicylaldehyde in a yield of 27%: white powder; mp 235–236 °C; ^{1}H NMR (300 MHz, $CDCl_3$) δ (ppm): 3.67 (dd, 1H, J_1 = 11.4 Hz, J_2 = 17.3 Hz, 1-Ha), 3.81 (dd, 1H, J_1 = 9.2 Hz, J_2 = 17.3 Hz, 1-Hb), 3.87 (s, 3H, CH_3O), 4.45 (d, 1H, J = 16.6 Hz, 6-Ha), 5.02 (d, 1H, J = 16.6 Hz, 6-Hb), 5.93 (dd, 1H, J_1 = 9.3 Hz, J_2 = 11.2 Hz, 11b-H), 6.92–7.95 (7H, Ar-H); ^{13}C NMR (75 MHz, $CDCl_3$) δ (ppm): 35.6 (1-C), 55.5 (CH_3O), 55.9 (11b-C), 72.8 (6-C), 114.2 (2C), 122.8, 122.9, 125.2, 129.1 (2C), 130.4, 130.5, 132.6, 155.7 (2-C), 156.5, 162.0, 164.0. TOF-HRMS: m/z $[M+H]^+$ calcd for $C_{18}H_{16}ClN_2O_3$: 343.0844; found: 343.0845.

4.2.10. 10-Chloro-2-*p*-tolyl-1,11b-dihydro-pyrazolo[1,5-*d*][1,4]benzoxazepin-5(6*H*)-one (3j)

The title compound was prepared from *p*-methyl-phenyl methyl ketone and 5-chloro-salicylaldehyde in a yield of 20%: white powder; mp 214–215 °C; ^{1}H NMR (300 MHz, $CDCl_3$) δ (ppm): 2.42 (s, 3H, CH_3), 3.68 (dd, 1H, J_1 = 11.4 Hz, J_2 = 17.4 Hz, 1-Ha), 3.82 (dd, 1H, J_1 = 9.2 Hz, J_2 = 17.4 Hz, 1-Hb), 4.46 (d, 1H, J = 16.6 Hz, 6-Ha), 5.02 (d, 1H, J = 16.6 Hz, 6-Hb), 5.94 (dd, 1H, J_1 = 9.6 Hz, J_2 = 11.3 Hz, 11b-H), 7.12–7.86 (7H, Ar-H); ^{13}C NMR (75 MHz, $CDCl_3$) δ (ppm): 21.6 (CH_3), 35.6 (1-C), 55.9 (11b-C), 72.8 (6-C), 122.8, 125.2, 127.3 (2C), 127.5, 129.5 (2C), 130.4, 130.5, 132.5, 141.7, 156.0 (2-C), 156.5, 164.1. TOF-HRMS: m/z $[M+H]^+$ calcd for $C_{18}H_{16}ClN_2O_2$: 327.0895; found: 327.0897.

4.2.11. 10-Chloro-2-phenyl-1,11b-dihydro-pyrazolo[1,5-*d*][1,4]benzoxazepin-5(6*H*)-one (3k)

The title compound was prepared from phenyl methyl ketone and 5-chloro-salicylaldehyde in a yield of 24%: white powder; mp 220–221 °C; ^{1}H NMR (300 MHz, $CDCl_3$) δ (ppm): 3.70 (dd, 1H, J_1 = 11.4 Hz, J_2 = 17.4 Hz, 1-Ha), 3.84 (dd, 1H, J_1 = 9.2 Hz, J_2 = 17.4 Hz, 1-Hb), 4.46 (d, 1H, J = 16.6 Hz, 6-Ha), 5.02 (d, 1H, J = 16.6 Hz, 6-Hb), 5.96 (dd, 1H, J_1 = 9.5 Hz, J_2 = 11.2 Hz, 11b-H), 7.12–7.96 (8H, Ar-H). TOF-HRMS: m/z $[M+H]^+$ calcd for $C_{17}H_{14}ClN_2O_2$: 313.0644; found: 313.0737.

4.2.12. 10-Chloro-2-(4-chloro-phenyl)-1,11b-dihydro-pyrazolo[1,5-*d*][1,4]benzoxazepin-5(6*H*)-one (3l)

The title compound was prepared from 4-chloro-phenyl methyl ketone and 5-chloro-salicylaldehyde in a yield of 21%: yellow powder; mp 206–207 °C; ^{1}H NMR (300 MHz, $CDCl_3$) δ (ppm): 3.67 (dd, 1H, J_1 = 11.5 Hz, J_2 = 17.4 Hz, 1-Ha), 3.82 (dd, 1H, J_1 = 9.3 Hz, J_2 = 17.4 Hz, 1-Hb), 4.46 (d, 1H, J = 16.7 Hz, 6-Ha), 5.03 (d, 1H, J = 16.7 Hz, 6-Hb), 5.98 (dd, 1H, J_1 = 9.4 Hz, J_2 = 11.2 Hz, 11b-H), 7.14–7.92 (7H, Ar-H). TOF-HRMS: m/z $[M+H]^+$ calcd for $C_{17}H_{13}Cl_2N_2O_2$: 347.0349; found: 347.0349.

4.2.13. 10-Chloro-2-(4-fluoro-phenyl)-1,11b-dihydro-pyrazolo[1,5-*d*][1,4]benzoxazepin-5(6*H*)-one (3m)

The title compound was prepared from 4-fluoro-phenyl methyl ketone and 5-chloro-salicylaldehyde in a yield of 25%: colorless crystals; mp 224–225 °C; ^{1}H NMR (300 MHz, $CDCl_3$) δ (ppm): 3.68 (dd, 1H, J_1 = 11.5 Hz, J_2 = 17.4 Hz, 1-Ha), 3.82 (dd, 1H, J_1 = 9.3 Hz, J_2 = 17.4 Hz, 1-Hb), 4.46 (d, 1H, J = 16.7 Hz, 6-Ha), 5.03 (d, 1H, J = 16.7 Hz, 6-Hb), 5.97 (dd, 1H, J_1 = 9.6 Hz, J_2 = 11.2 Hz, 11b-H), 7.10–7.97 (7H, Ar-H). TOF-HRMS: m/z $[M+H]^+$ calcd for $C_{17}H_{13}ClFN_2O_2$: 331.0644; found: 331.0645.

4.2.14. 10-Chloro-2-(2-fluoro-phenyl)-1,11b-dihydro-pyrazolo[1,5-*d*][1,4]benzoxazepin-5(6*H*)-one (3n)

The title compound was prepared from 2-fluoro-phenyl methyl ketone and 5-chloro-salicylaldehyde in a yield of 21%: yellow

powder; mp 219–221 °C; ^{1}H NMR (300 MHz, $CDCl_3$) δ (ppm): 3.81 (ddd, 1H, J_1 = 3.0 Hz, J_2 = 11.5 Hz, J_3 = 18.3 Hz, 1-Ha), 3.95 (ddd, 1H, J_1 = 2.6 Hz, J_2 = 9.3 Hz, J_3 = 18.3 Hz, 1-Hb), 4.47 (d, 1H, J = 16.7 Hz, 6-Ha), 5.04 (d, 1H, J = 16.7 Hz, 6-Hb), 5.96 (m, 1H), 7.11–8.22 (7H, Ar-H). TOF-HRMS: m/z $[M+H]^+$ calcd for $C_{17}H_{13}ClFN_2O_2$: 331.0644; found: 331.0643.

4.2.15. 8,10-Dibromo-2-(4-methoxy-phenyl)-1,11b-dihydro-pyrazolo[1,5-*d*][1,4]benzoxazepin-5(6*H*)-one (3o)

The title compound was prepared from 4-methoxy-phenyl methyl ketone and 3,5-dibromo-salicylaldehyde in a yield of 20%: white powder; mp 269–270 °C; ^{1}H NMR (300 MHz, DMSO-d_6) δ (ppm): 3.75 (dd, 1H, J_1 = 11.6 Hz, J_2 = 17.8 Hz, 1-Ha), 3.87 (s, 1H), 3.99 (dd, 1H, J_1 = 8.6 Hz, J_2 = 17.8 Hz, 1-Hb), 4.44 (d, 1H, J = 16.5 Hz, 6-Ha), 5.02 (d, 1H, J = 16.5 Hz, 6-Hb), 6.02 (dd, 1H, J_1 = 8.8 Hz, J_2 = 11.3 Hz, 11b-H), 6.92–7.91 (6H, Ar-H); ^{13}C NMR (75 MHz, DMSO-d_6) δ (ppm): 40.5 (1-C), 60.3 (CH_3O), 60.9 (11b-C), 76.2 (6-C), 118.9 (2C), 121.7, 122.9, 127.7, 132.6, 134.0 (2C), 139.8, 140.4, 158.3 (2-C), 161.1, 166.6, 167.8. TOF-HRMS: m/z $[M+H]^+$ calcd for $C_{18}H_{15}Br_2N_2O_3$: 466.9425; found: 466.9426.

4.2.16. 2-(4-Methoxy-phenyl)-6-methyl-1,11b-dihydro-pyrazolo[1,5-*d*][1,4]benzoxazepin-5(6*H*)-one (3p)

The title compound was prepared from 4-methoxy-phenyl methyl ketone and salicylaldehyde in a yield of 26%: white powder; mp 240–241 °C; ^{1}H NMR (300 MHz, $CDCl_3$) δ (ppm): 1.55 (d, 3H, J = 6.8 Hz, CH_3), 3.75 (d, 1H, J = 2.2 Hz, 1-Ha), 3.78 (d, 1H, J = 2.7 Hz, 1-Hb), 3.86 (s, 3H, CH_3O), 5.05 (q, 1H, J = 6.8 Hz, 6-H), 5.92 (t, 1H, J = 10.6 Hz, 11b-H), 6.90–7.87 (8H, Ar-H); ^{13}C NMR (75 MHz, $CDCl_3$) δ (ppm): 17.4 (CH_3), 38.4 (1-C), 55.4 (CH_3O), 58.0 (11b-C), 76.1 (6-C), 114.1 (2C), 122.4, 123.3, 123.8, 126.1, 128.7, 128.9 (2C), 129.4, 155.3 (2-C), 155.8, 161.7, 167.1. TOF-HRMS: m/z $[M+H]^+$ calcd for $C_{19}H_{19}N_2O_3$: 323.1390; found: 323.1391.

4.2.17. 6-Methyl-2-p-tolyl-1,11b-dihydro-pyrazolo[1,5-*d*][1,4]benzoxazepin-5(6*H*)-one (3q)

The title compound was prepared from *p*-methyl-phenyl methyl ketone and salicylaldehyde in a yield of 28%: white powder; mp 195–196 °C; ^{1}H NMR (300 MHz, $CDCl_3$) δ (ppm): 1.55 (d, 3H, J = 6.8 Hz, CH_3), 2.40 (s, 3H, CH_3), 3.76 (d, 1H, J = 2.8 Hz, 1-Ha), 3.79 (d, 1H, J = 3.5 Hz, 1-Hb), 5.05 (q, 1H, J = 6.8 Hz, 6-H), 5.93 (t, 1H, J = 10.6 Hz, 11b-H), 7.03–7.83 (8H, Ar-H). TOF-HRMS: m/z $[M+H]^+$ calcd for $C_{19}H_{19}N_2O_2$: 307.1441; found: 307.1441.

4.2.18. 6-Methyl-2-phenyl-1,11b-dihydro-pyrazolo[1,5-*d*][1,4]benzoxazepin-5(6*H*)-one (3r)

The title compound was prepared from phenyl methyl ketone and salicylaldehyde in a yield of 25%: white powder; mp 258–259 °C; ^{1}H NMR (300 MHz, $CDCl_3$) δ (ppm): 1.55 (d, 3H, J = 6.8 Hz, CH_3), 3.78 (d, 1H, J = 3.2 Hz, 1-Ha), 3.81 (d, 1H, J = 3.8 Hz, 1-Hb), 5.05 (q, 1H, J = 6.8 Hz, 6-H), 5.96 (t, 1H, J = 10.6 Hz, 11b-H), 7.03–7.93 (9H, Ar-H). TOF-HRMS: m/z $[M+H]^+$ calcd for $C_{18}H_{17}N_2O_2$: 293.1285; found: 293.1297.

4.2.19. 2-(4-Chloro-phenyl)-6-methyl-1,11b-dihydro-pyrazolo[1,5-*d*][1,4]benzoxazepin-5(6*H*)-one (3s)

The title compound was prepared from 4-chloro-phenyl methyl ketone and salicylaldehyde in a yield of 20%: yellow powder; mp 182–184 °C; ^{1}H NMR (300 MHz, $CDCl_3$) δ (ppm): 1.55 (d, 3H, J = 6.8 Hz, CH_3), 3.75 (d, 1H, J = 3.2 Hz, 1-Ha), 3.79 (d, 1H, J = 3.8 Hz, 1-Hb), 5.05 (q, 1H, J = 6.8 Hz, 6-H), 5.96 (t, 1H, J = 10.7 Hz, 11b-H), 7.05–7.88 (8H, Ar-H); ^{13}C NMR (75 MHz, $CDCl_3$) δ (ppm): 17.3 (CH_3), 38.4 (1-C), 58.3 (11b-C), 76.1 (6-C), 122.4, 123.9, 126.1, 128.3, 128.4 (2C), 129.0 (2C), 129.2, 129.5, 136.9, 155.1 (2-C), 155.2, 167.4. TOF-HRMS: m/z $[M+H]^+$ calcd for $C_{18}H_{16}ClN_2O_2$: 327.0895; found: 327.0890.

4.2.20. 2-(2-Chloro-phenyl)-6-methyl-1,11b-dihydro-pyrazolo[1,5-*d*][1,4]benzoxazepin-5(6*H*)-one (3t)

The title compound was prepared from 2-chloro-phenyl methyl ketone and salicylaldehyde in a yield of 28%: white crystals; mp 173–175 °C; ^{1}H NMR (300 MHz, $CDCl_3$) δ (ppm): 1.56 (d, 3H, J = 6.8 Hz, CH_3), 3.89–4.10 (m, 2H, 1-Ha, 1-Hb), 5.05 (q, 1H, J = 6.8 Hz, 6-H), 5.97 (t, 1H, J = 10.8 Hz, 11b-H), 7.05–7.93 (8H, Ar-H). TOF-HRMS: m/z $[M+H]^+$ calcd for $C_{18}H_{16}ClN_2O_2$: 327.0895; found: 327.0894.

4.2.21. 2-(4-Fluoro-phenyl)-6-methyl-1,11b-dihydro-pyrazolo[1,5-*d*][1,4]benzoxazepin-5(6*H*)-one (3u)

The title compound was prepared from 4-fluoro-phenyl methyl ketone and salicylaldehyde in a yield of 21%: white powder; mp 189–190 °C; ^{1}H NMR (300 MHz, $CDCl_3$) δ (ppm): 1.55 (d, 3H, J = 6.8 Hz, CH_3), 3.76 (d, 1H, J = 2.1 Hz, pyrazole 4-Ha), 3.79 (d, 1H, J = 2.7 Hz, pyrazole 4-Hb), 5.05 (q, 1H, J = 6.8 Hz, oxazepane 2-H), 5.96 (t, 1H, J = 10.7 Hz, pyrazole 5-H), 7.04–7.94 (8H, Ar-H). TOF-HRMS: m/z $[M+H]^+$ calcd for $C_{18}H_{16}FN_2O_2$: 311.1190; found: 311.1186.

4.3. Crystal structure determination for compounds 3e, 3m and 3t

X-ray single-crystal diffraction data for compounds **3e**, **3m** and **3t** was collected on a Bruker SMART APEX CCD diffractometer at 293(2) K using MoKα radiation (λ = 0.71073 Å) by the ω scan mode. The program SAINT was used for integration of the diffraction profiles. The structure was solved by direct methods using the SHELXS program of the SHELXTL package and refined by full-matrix least-squares methods with SHELXL.[30] The corrections for *LP* factors were applied. Multi-scan symmetry-related measurement was used as experimental absorption correction type. The non-hydrogen atoms of compounds **3e**, **3m** and **3t** were refined with anisotropic thermal parameters whereas all hydrogen atoms were generated theoretically onto the parent atoms and refined isotropically with fixed thermal factors.

4.4. Enzymatic assay

Enzymatic hMAO-A and hMAO-B activity of compounds was determined by a fluorimetric method.[22] Briefly, 0.1 mL of sodium phosphate buffer (0.05 M, pH 7.4) containing various concentrations of the test drugs (new compounds or reference inhibitors). The appropriate amounts of recombinant hMAO-A or hMAO-B was adjusted to the same reaction velocity in the presence of both isoforms the same concentration of substrate: 165 pmol of *p*-tyramine/min (hMAO-A: 1.1 μg protein; specific activity: 150 nmol of *p*-tyramine oxidized top hydroxyphenylacetaldehyde/min/mg protein; hMAO-B: 7.5 μg protein; specific activity: 22 nmol of *p*-tyramine transformed/min/mg protein). The mixture was incubated for 15 min at 37 °C, placed in the dark fluorimeter chamber. After this incubation period, the reaction was started by adding 200 μM of 10-acetyl-3,7-dihydroxyphenoxazine reagent (Amplex Red assay kit, Molecular Probes, Inc., Eugene, OR), 1 U/mL horseradish peroxidase, and 1 mM *p*-tyramine. The production of H_2O_2 and, consequently, of resorufin, was quantified at 37 °C in a multidetection microplate fluorescence reader based on the fluorescence generated (excitation, 545 nm, emission, 590 nm) over a 15 min period, during which the fluorescence increased linearly.

4.5. Molecular modeling

The compounds described in this article were treated first by LigPrep 2.6 in the Schrödinger suite, and then docked into the active site of the hMAO-B (PDB code: 2V5Z) by employing the program of Glide 6.7 of Schrödinger suite. Both of standard precision (SP) and extra precision (XP) of Glide were tested and finally the results from the SP were used. The final docked complexes were done a quick molecular dynamic simulation using the MC/SD module of MarcoModel in the Schrödinger suite.

Acknowledgments

This work was supported by the National Natural Science Foundation of China (21572003), Natural Science Foundation of Anhui Higher Education Institutions (KJ2016A339) and National Training Programs of Innovation and Entrepreneurship for Undergraduates (201410366041).

Supplementary data

Crystallographic data (excluding structure factors) for the structure had been deposited with the Cambridge Crystallographic Data Center as supplementary publication Nos. CCDC 1428287 (**3e**), 1040100 (**3m**) and 1040101 (**3t**). These data can be obtained free of charge via the URL http://www.ccdc.cam.ac.uk (or from the CCDC, 12 Union Road, Cambridge CB2 1EZ, UK; fax: (+44) 1223 336033; e-mail: deposit@ccdc.cam.ac.uk). Supplementary data (representative ^{1}H and ^{13}C NMR spectra of compounds **3a**–**3u**) associated with this article can be found, in the online version, at http://dx.doi.org/10.1016/j.bmc.2016.02.045.

References and notes

1. Binda, C.; Milczek, E. M.; Bonivento, D.; Wang, J.; Mattevi, A.; Edmondson, D. E. *Curr. Top. Med. Chem.* **2011**, *11*, 2788.
2. Shih, J. C.; Chen, K.; Ridd, M. J. *Annu. Rev. Neurosci.* **1999**, *22*, 197.
3. De Colibus, L.; Li, M.; Binda, C.; Lustig, A.; Edmondson, D. E.; Mattevi, A. *Proc. Natl. Acad. Sci. U.S.A.* **2005**, *102*, 12684.
4. Binda, C.; Newton-Vinson, P.; Hubalek, F.; Edmondson, D. E.; Mattevi, A. *Nat. Struct. Biol.* **2002**, *9*, 22.
5. Shulman, K. I.; Herrmann, N.; Walker, S. E. *CNS Drugs* **2013**, *27*, 789.
6. Carradori, S.; Secci, D.; Bolasco, A.; Chimenti, P.; D'Ascenzio, M. *Expert Opin. Ther. Pat.* **2012**, *22*, 759.
7. Youdim, M. B.; Edmondson, D.; Tipton, K. F. *Nat. Rev. Neurosci.* **2006**, *7*, 295.
8. Naoi, M.; Maruyama, W.; Inaba-Hasegawa, K. *Curr. Top. Med. Chem.* **2012**, *12*, 2177.
9. Mallajosyula, J. K.; Kaur, D.; Chinta, S. J.; Rajagopalan, S.; Rane, A.; Nicholls, D. G.; Di Monte, D. A.; Macarthur, H.; Andersen, J. K. *PLoS One* **2008**, *3*, e1616.
10. Mishra, N.; Sasmal, D. *Brain Res.* **2012**, *1470*, 45.
11. Carradori, S.; Silvestri, R. *J. Med. Chem.* **2015**, *58*, 6717.
12. Secci, D.; Carradori, S.; Bolasco, A.; Bizzarri, B.; D'Ascenzio, M.; Maccioni, E. *Curr. Top. Med. Chem.* **2012**, *12*, 2240.
13. Binda, C.; Wang, J.; Pisani, L.; Caccia, C.; Carotti, A.; Salvati, P.; Edmondson, D. E.; Mattevi, A. *J. Med. Chem.* **2007**, *50*, 5848.
14. Secci, D.; Bolasco, A.; Carradori, S.; D'Ascenzio, M.; Nescatelli, R.; Yáñez, M. *Eur. J. Med. Chem.* **2012**, *58*, 405.
15. Pan, Z. X.; He, X.; Chen, Y. Y.; Tang, W. J.; Shi, J. B.; Tang, Y. L.; Song, B. A.; Li, J.; Liu, X. H. *Eur. J. Med. Chem.* **2014**, *80*, 278.
16. Ruan, B.-F.; Cheng, H.-J.; Ren, J.; Li, H.-L.; Guo, L.-L.; Zhang, X.-X.; Liao, C. *Eur. J. Med. Chem.* **2015**, *103*, 185.
17. Farina, R.; Pisani, L.; Catto, M.; Nicolotti, O.; Gadaleta, D.; Denora, N.; Soto-Otero, R.; Mendez-Alvarez, E.; Passos, C. S.; Muncipinto, G.; Altomare, C. D.; Nurisso, A.; Carrupt, P. A.; Carotti, A. *J. Med. Chem.* **2015**, *58*, 5561.
18. Pisani, L.; Catto, M.; Nicolotti, O.; Grossi, G.; Di Braccio, M.; Soto-Otero, R.; Mendez-Alvarez, E.; Stefanachi, A.; Gadaleta, D.; Carotti, A. *Eur. J. Med. Chem.* **2013**, *70*, 723.
19. Pisani, L.; Farina, R.; Nicolotti, O.; Gadaleta, D.; Soto-Otero, R.; Catto, M.; Di Braccio, M.; Mendez-Alvarez, E.; Carotti, A. *Eur. J. Med. Chem.* **2015**, *89*, 98.
20. Tong, X.; Chen, R.; Zhang, T. T.; Han, Y.; Tang, W. J.; Liu, X. H. *Bioorg. Med. Chem.* **2015**, *23*, 515.
21. Liu, X. H.; Jia, Y. M.; Song, B. A.; Pang, Z. X.; Yang, S. *Bioorg. Med. Chem. Lett.* **2013**, *23*, 720.
22. Santana, L.; Gonzalez-Diaz, H.; Quezada, E.; Uriarte, E.; Yanez, M.; Vina, D.; Orallo, F. *J. Med. Chem.* **2008**, *51*, 6740.
23. Fernandez, H. H.; Chen, J. J. *Clin. Neuropharmacol.* **2007**, *30*, 150.
24. Liao, C.; Sitzmann, M.; Pugliese, A.; Nicklaus, M. C. *Future Med. Chem.* **2011**, *3*, 1057.
25. *Glide, version 6.7*; Schrödinger, LLC: New York, NY, 2015.
26. Bonivento, D.; Milczek, E. M.; McDonald, G. R.; Binda, C.; Holt, A.; Edmondson, D. E.; Mattevi, A. *J. Biol. Chem.* **2010**, *285*, 36849.
27. Hernandes, M. Z.; Cavalcanti, S. M.; Moreira, D. R.; de Azevedo Junior, W. F.; Leite, A. C. *Curr. Drug Targets* **2010**, *11*, 303.
28. Son, S. Y.; Ma, A.; Kondou, Y.; Yoshimura, M.; Yamashita, E.; Tsukihara, T. *Proc. Natl. Acad. Sci. U.S.A.* **2008**, *105*, 5739.
29. Liao, C. Z.; Yao, R. S. *Sci. China Chem.* **2013**, *56*, 1392.
30. Sheldrick, G. M. *SHELXTL-97, Program for Crystal Structure Solution and Refinement*; University of Göttingen: Göttingen, Germany, 1997.